J Biomol NMR (2011) 50:129–136
DOI 10.1007/s10858-011-9501-9

ARTICLE

Sensitive ^{13}C–^{13}C correlation spectra of amyloid fibrils at very high spinning frequencies and magnetic fields

Markus Weingarth · Yuichi Masuda · K. Takegoshi · Geoffrey Bodenhausen · Piotr Tekely

Received: 24 January 2011 / Accepted: 9 March 2011 / Published online: 29 March 2011

Abstract Sensitive 2D solid-state ^{13}C–^{13}C correlation spectra of amyloid β fibrils have been recorded at very fast spinning frequencies and very high magnetic fields. It is demonstrated that PARIS-xy recoupling using moderate *rf* amplitudes can provide structural information by promoting efficient magnetization transfer even under such challenging experimental conditions. Furthermore, it has been shown both experimentally and by numerical simulations that the method is not very sensitive to dipolar truncation effects and can reveal direct transfer across distances of about 3.5–4Å.

Keywords Amyloid β fibrils · Solid-state NMR · ^{13}C–^{13}C 2D correlation spectra · Dipolar truncation · PARIS-xy dipolar recoupling · Ultra-high magnetic field

Electronic supplementary material The online version of this article (doi:10.1007/s10858-011-9501-9) contains supplementary material, which is available to authorized users.

M. Weingarth · G. Bodenhausen · P. Tekely (✉)
Département de Chimie, Ecole Normale Supérieure,
24 rue Lhomond, 75231 Paris, France
e-mail: piotr.tekely@ens.fr

M. Weingarth · G. Bodenhausen · P. Tekely
Université Pierre et Marie Curie, 4 Place Jussieu,
75005 Paris, France

M. Weingarth · G. Bodenhausen · P. Tekely
Département de Chimie, CNRS, UMR 7203, 24 rue Lhomond,
75005 Paris, France

Present Address:
M. Weingarth
Utrecht University, Padualaan 8, 3584 CH Utrecht,
The Netherlands

Y. Masuda · K. Takegoshi
Department of Chemistry, Graduate School of Science,
Kyoto University, Kyoto 606-8502, Japan

Introduction

High resolution solid-state NMR permits detailed studies of structures and dynamics of biomolecules and their aggregates in microcrystalline and non-crystalline forms (Castellani et al. 2002; Rienstra et al. 2002; Lange et al. 2005). NMR holds promise as a powerful method to study peptides and proteins in membranes (Lange et al. 2006; Cady et al. 2010) or amyloid fibrils peptides (Petkova et al. 2005; Iwata et al. 2006; Chimon et al. 2007; Nielsen et al. 2009; Masuda et al. 2009), since there are currently no other means to study their structures and dynamics at an atomic level. Spectral assignment of ^{13}C or ^{15}N resonances through scalar couplings or by recoupling dipolar interactions constitutes an initial step towards the determination of atomic distances and torsion angles. Low sensitivity is the primary limitation for complex biological systems in low concentrations. Very high magnetic fields and very fast magic angle spinning (MAS) can provide sufficient sensitivity and spectral resolution (Laage et al. 2009; Sperling et al. 2010). However, solid-state NMR recoupling experiments at these extreme conditions are very challenging due to the large dispersion of the isotropic chemical shifts and the efficient averaging of dipolar interactions.

In this paper we show that the recently developed PARIS-xy method for dipolar recoupling (Weingarth et al. 2010a) allows one to record sensitive 2D ^{13}C–^{13}C correlation spectra of as little as 1 mg of samples of amyloid β fibrils at very high spinning frequencies ($40 < \nu_{rot} < 60$ kHz) at the highest available static magnetic fields (900 and 1,000 MHz

for protons). Furthermore, we demonstrate experimentally and by numerical simulations that the method is not very sensitive to dipolar truncation and can reveal direct transfer across distances of about 3.5–4 Å.

Materials and methods

Synthesis of Aβ42 peptides

The samples were synthesized in a stepwise fashion on 0.1 mmol of Fmoc-L-alanine-polyethylene glycol-polystyrene support resin by Pioneer^{TM} as reported previously (Irie et al. 1998; Murakami et al. 2002). The coupling reaction was carried out using Fmoc protected amino acids (0.4 mmol), HATU (0.4 mmol), and DIPEA (0.8 mmol) in DMF for 30 min. After each coupling reaction, the Fmoc group at the N-terminus was removed with 20% piperidine in DMF. After chain elongation, the peptide resin was washed with DMF and CH_2Cl_2 treated with a cocktail containing trifluoroacetic acid, *m*-cresol, ethanedithiol, and thioanisole for final deprotection and cleavage from the resin. After shaking at room temperature for 2 h, the crude peptide was precipitated by diethyl ether and purified by HPLC under alkaline conditions as reported previously (Murakami et al. 2002). Lyophilization gave Aβ42, the purity of which was confirmed by HPLC (>98%). The total yields were about 9%. We prepared two samples (see Supporting Material Figure S1): sample I is uniformly ^{13}C- and ^{15}N-labeled at F20 and selectively ^{13}C-labeled at the C$^{\beta}$ of A21 to probe to what extent PARIS-xy is sensitive to dipolar truncation; sample II is uniformly ^{13}C- and ^{15}N- labeled at V24 and selectively ^{13}C-labeled at the carbonyl C′ carbon of D23. The synthesized peptides exhibited satisfactory mass spectra obtained by MALDI-TOF–MS (see Supporting Material Figure S2) of sample I (MH^+, average molecular mass; observed 4,525.72, calculated 4,526.00) and sample II (MH^+, average molecular mass; observed 4,521.90, calculated 4,522.12). For other details of synthesis see Supporting Material.

Fibril formation

Aβ42 peptide was dissolved in 0.1% NH_4OH at a concentration of 250 μM. After a tenfold dilution in 50 mM sodium phosphate containing 100 mM NaCl at pH 7.1, the resulting peptide solution (25 μM, pH 7.4) was incubated under quiescent conditions at 37°C for 48 h. White aggregates like wet cotton appeared. After centrifugation at 17.712 g and 4°C, followed by washing with distilled water, the resultant aggregates were dried in vacuo. The amount of sample used for solid-state NMR was about 1 mg.

Transmission electron micrographs of a negatively stained preparations of fibrils formed by Aβ42

The formation of fibrils of Aβ42 was confirmed by electron microscopy (Figure S3). The incubation conditions were the same for preparing samples for solid-state NMR. Each Aβ42 peptide was dissolved in 0.1% NH_4OH to 250 μM. After a tenfold dilution with 50 mM sodium phosphate containing 100 mM NaCl at pH 7.1, the resultant peptide solution (25 μM, pH 7.4) was again incubated at 37°C for 48 h. After centrifugation, the supernatant was removed from the pellets. Aggregates were suspended in distilled water by gentle vortex mixing. The suspensions were applied to a 200-mesh Formvar-coated copper grid (Nissin EM, Tokyo, Japan) and dried in air before negative staining for a few seconds with 2% uranyl acetate. The fibrils were examined with a HITACHI H-7650 transmission electron microscope.

NMR experiments

All experiments were carried out on 900 and 1,000 MHz BRUKER AVANCE III spectrometers with 1.3 mm BRUKER probes. The ^{13}C chemical shifts were referenced with respect to the C′ chemical shift (δ_{iso} = 176.5 ppm) of α-glycine (Potrzebowski et al. 1998) used as an external reference. For 2D ^{13}C–^{13}C experiments, the phase-alternated recoupling irradiation scheme with orthogonal phases (PARIS-xy) (Weingarth et al. 2010a; Fig. 1) was used during the mixing period. PARIS-xy irradiation consists of a block of *m* pairs of phase-alternated pulses $[(x)(-x)]_m$, followed by a phase-shifted block $[(y)(-y)]_m$ with pulse durations equal to half a rotor period $\tau_p = \tau_{rot}/2$. This leads to broadening and overlap between spectrally close resonances like aliphatic carbons. By choosing $m = 1$ or 2, modulation sidebands (MS) that roughly match chemical shift differences also permit the exchange of magnetization between spectrally distant carbons (Weingarth et al. 2010a). The choice of *m* offers an easy way to control magnetization transfer: $m = 1$ leads to sidebands at $\pm 0.5\nu_{rot}$, while $m = 2$ generates two sets of sidebands at $\pm 0.5\nu_{rot}$ and $\pm 0.75\nu_{rot}$. Even with moderate *rf* amplitudes, the PARIS-xy method can promote both broadband and band-selective transfer of longitudinal magnetization between chemically inequivalent ^{13}C spins. To achieve dipolar recoupling, the *rf* irradiation is applied only to protons, thus avoiding losses of ^{13}C magnetization that is not subjected to any *rf* irradiation. PISSARRO heteronuclear decoupling (Weingarth et al. 2008a, 2009b, 2011) was applied during the evolution and detection intervals.

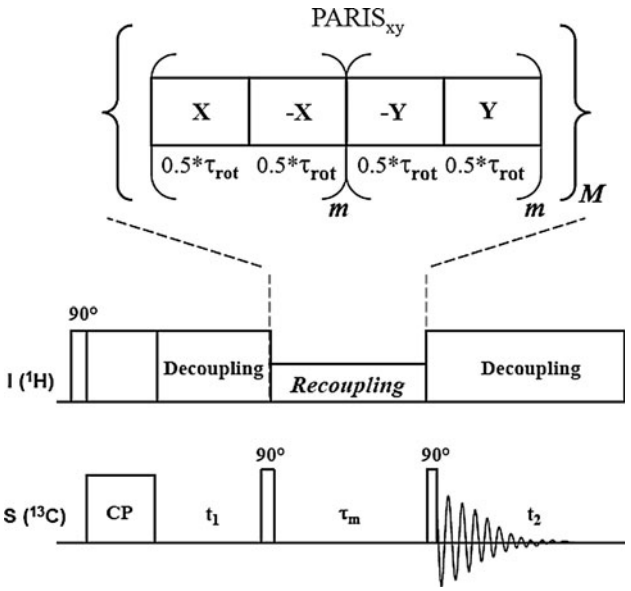

Fig. 1 Pulse sequence used in this work for polarization transfer between carbon-13 nuclei in Aβ42 fibrils

Numerical simulations

The numerical simulations were carried out with the SPINEVOLUTION program (Veshtort and Griffin 2006). As a model spin-system we first used a $C^{\alpha}H^{\alpha}C^{\beta}H^{\beta}H^{\beta}H^{N}H^{N}CO$ fragment based on L-serine, which is representative for most amino acids. For this model system all simulations were done at 14.1 T (600 MHz), $\nu_{rot} = 40$ kHz, *rf* recoupling amplitude $\nu_1^H = 26.66$ kHz with PARIS-xy irradiation ($m = 1$), assuming ideal decoupling during signal detection. The proton chemical shift anisotropy (CSA) tensors (5 ppm for each proton) were arbitrarily oriented. Further simulations assumed a model fragment with 9 spins (see Supporting Material Figure S3) of the amyloid Aβ peptide 42 extracted from a structural model (Lührs et al. 2005). Although a variety of structural models of Aβ fibrils has been proposed (Lührs et al. 2005; Petkova et al. 2002; Tycko 2006; Masuda et al. 2009; Ahmed et al. 2010), there is a general consensus that the amino acid residues at positions 17–21 form an intermolecular parallel beta-sheet. These simulations were run at conditions close to those used in experiments: $\nu_1^H = 30$ kHz, $\nu_{rot} = 50$ kHz, 1,000 MHz proton frequency, $\tau_m = 400$ ms, $m = 2$. The six protons taken into account were the closest to the A21$^{\beta}$ carbon. The chemical shift difference between F20^{CO} and A21$^{\beta}$ is equal to 37.5 kHz, and matches the position of the outer modulation sideband $\nu_{mod} = \frac{3}{4}\nu_{rot}$. A 5 ppm CSA tensor was assumed for each proton with an arbitrary orientation. Perfect decoupling during both t_1 and t_2 intervals was assumed.

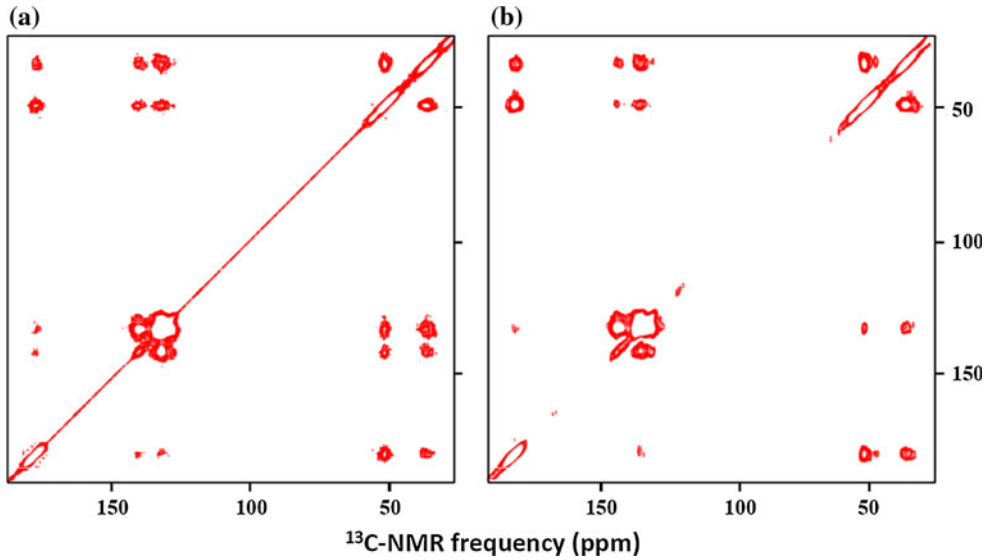

Fig. 2 ^{13}C–^{13}C correlation spectra of Aβ42 fibrils (sample I) recorded at $B_0 = 21.1$ T (900 MHz for protons) with PARIS-xy recoupling : **a** $\nu_{rot} = 39$ kHz, $m = 1$, mixing time $\tau_m = 300$ ms, proton recoupling *rf* amplitude $\nu_1^H = 15$ kHz, acquisition time in the indirect dimension $t_1^{max} = 1.4$ ms, 340 scans per increment, recycle delay 2.8 s for a total experimental time of 21 h; **b** $\nu_{rot} = 40$ kHz, $m = 2$, $\tau_m = 300$ ms, $\nu_1^H = 25$ kHz, acquisition time in the indirect dimension $t_1^{max} = 1.34$ ms, 400 scans per increment, recycle delay 2.8 s for a total experimental time of 24 h. Both spectra were processed with a covariance method. The superposition of covariance and FT processed spectra is shown in Fig. S5

Results and discussion

Figure 2 shows 2D ^{13}C–^{13}C correlation spectra of sample I recorded at 21.2 T (900 MHz ^{1}H-frequency), illustrating PARIS-xy's ability to promote broadband polarization transfer between spectrally distant regions. The spectra were processed by a covariance method, thus allowing one to reduce t_1^{max}, which makes it possible to record more scans for each t_1 increment (Weingarth et al. 2010b). The recoupling results in magnetization exchange between all three types of carbons, so that all possible intra-residual contacts within F20 appear. The possibility of promoting an efficient transfer between aromatic and aliphatic carbons opens the way for systems where aromatic residues are located in hydrophobic cavities or in gates like in the M2-channel (Cady et al. 2010).

The cross-sections in Fig. 3 extracted from the 2D FT processed ^{13}C–^{13}C correlation spectra show that PARIS-xy recoupling with $m = 1$ (a, b) or $m = 2$ (c, d) led to high polarization transfer efficiency (defined as the sum of cross-peaks amplitudes $\Sigma a_{SS'}$ ($\tau_m > 0$) divided by diagonal peak amplitude a_{SS} ($\tau_m = 0$) in the same row) between 42 and 63%, despite relatively low recoupling amplitudes $\nu_1^H = 15$ kHz (a, b) and 25 kHz (c, d). The fraction of the transferred polarization was found to reflect the relevant intra-residual distances. Switching from $m = 2$ to 1 enhances the transfer between aliphatic and aromatic carbons considerably. Indeed, $m = 1$ yields only one set of modulation sidebands which promote the magnetization exchange mainly between two regions, while $m = 2$ offers two sets of modulation sidebands which leads to a more uniform transfer over the entire spectral window. It is also worth to point out that at a higher spinning frequency $\nu_1^H = 57$ kHz with $m = 1$, the transfer between carbonyl and aliphatic carbons is clearly favoured (see Fig. S4 in Supporting Material). The line widths and chemical shifts

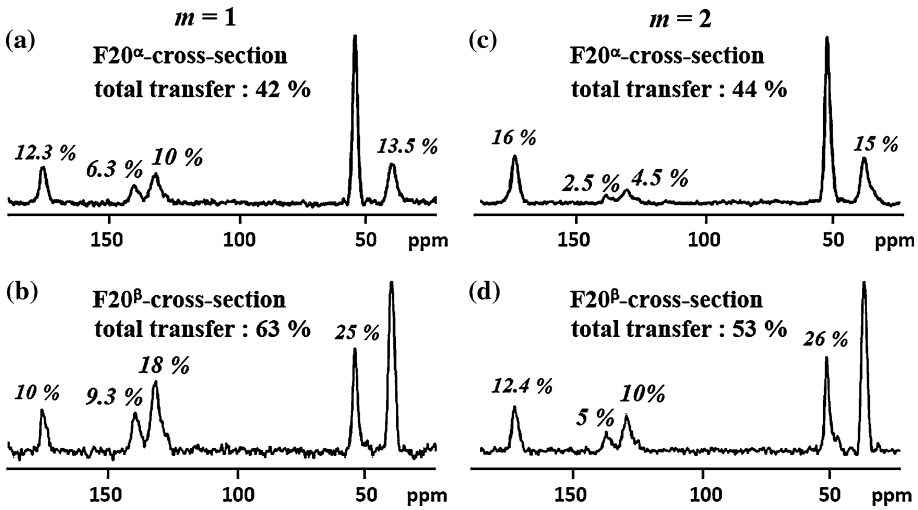

Fig. 3 Cross-sections extracted from 2D FT processed ^{13}C–^{13}C correlation spectra of Aβ42 fibrils (sample I) recorded with PARIS-xy recoupling using $m = 1$ (**a**, **b**) or $m = 2$ (**c**, **d**) with the same acquisition parameters as in Fig. 2

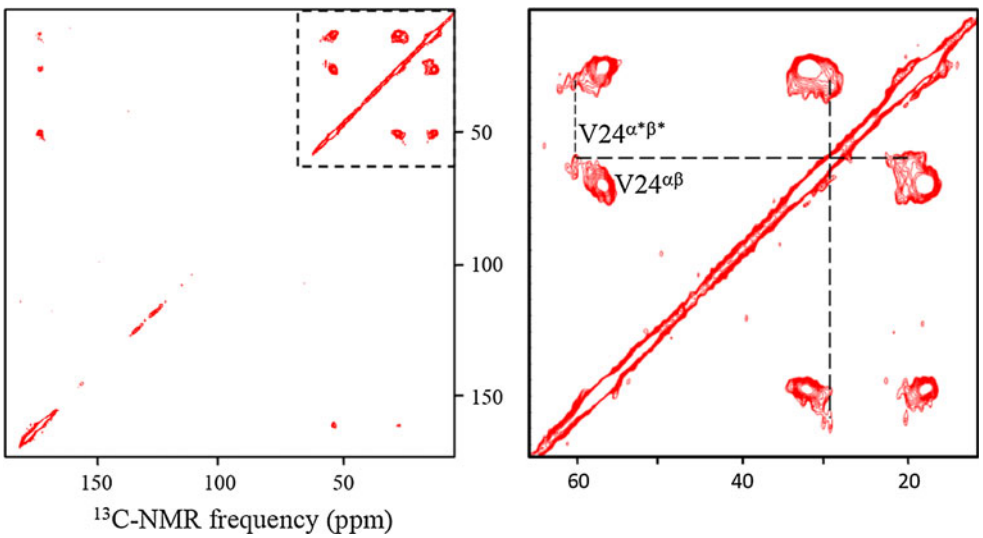

Fig. 4 (*Left*) PARIS-xy broadband 2D ^{13}C–^{13}C correlation spectrum of sample II selectively ^{13}C-labeled at the C' of D23 and uniformly ^{13}C- and ^{15}N-labeled in V24. The spectrum was recorded at 21.1 T (900 MHz for protons), $\nu_{rot} = 45$ kHz, $m = 2$, $\nu_1^H = 26$ kHz, $\tau_m = 300$ ms, $t_1^{max} = 1.79$ ms, 645 scans per increment, recycle delay 2.8 s, processed by 2D Fourier transformation. (*Right*) Expansion revealing the presence of two different conformations involving V24$^{\alpha}$ and V24$^{\beta}$

of some selected resonances of sample I are given in Table S1 (Supporting Material.) The recorded line widths were slightly larger than those of the shorter Aβ40 fibrils measured by Tycko's group (Petkova et al. 2005). Since Aβ42 aggregates more rapidly than Aβ40, the Aβ42 fibrils are expected to be less uniform than Aβ40 fibrils. As discussed below, we observed two sets of chemical shifts for some residues, which may suggest that Aβ42 forms at least two polymorphs. The chemical shift values of the major species are close to those reported for Aβ40 fibrils (Petkova et al. 2005; Chimon et al. 2007). The presence of a minor species might be related to different type of fibrils or to amorphous aggregates that were not found in EM images, probably due to their low concentration.

A PARIS-xy broadband 2D ^{13}C–^{13}C correlation spectrum of sample II selectively ^{13}C-labeled at the C′ of D23 and uniformly ^{13}C- and ^{15}N-labeled in V24 is shown in Fig. 4. The spectrum reveals all intra-residual contacts in V24. The residues at positions 23 and 24 could form a turn or bend structure (Petkova et al. 2005; Lührs et al. 2005; Masuda et al. 2008), though the precise structure of this region remains elusive. Furthermore, this spectrum reveals the presence of two different conformations involving V24$^{\alpha}$ and V24$^{\beta}$.

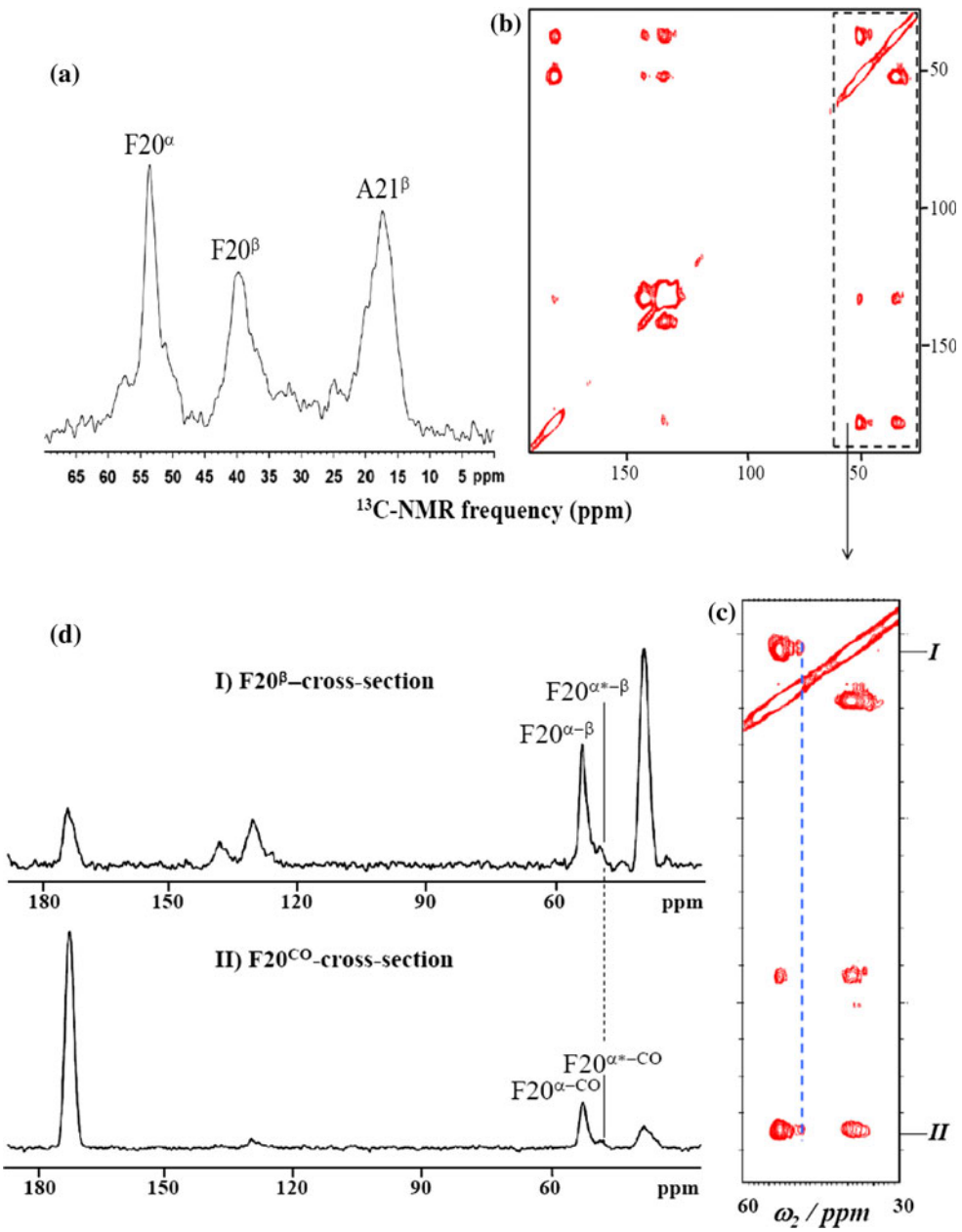

Fig. 5 **a** ^{13}C CP/MAS spectrum and **b** PARIS-xy correlation spectrum of sample I recorded at 21.2 T and $\nu_{rot} = 40$ kHz. The spectral region highlighted by a *dotted box* is expanded in **c**, showing the short connectivity walk through F20$^{\alpha*\text{-CO}}$ to F20$^{\alpha*\text{-}\beta}$. **d** Cross-sections of **c** for *I* F20$^{\beta}$ and *II* F20$^{\text{CO}}$ which show the presence of two different conformations involving F20$^{\alpha}$ through four well separated cross-peaks F20$^{\alpha\text{-CO}}$, F20C$^{\alpha*\text{-CO}}$, F20$^{\alpha\text{-}\beta}$ and F20C$^{\alpha*\text{-}\beta}$

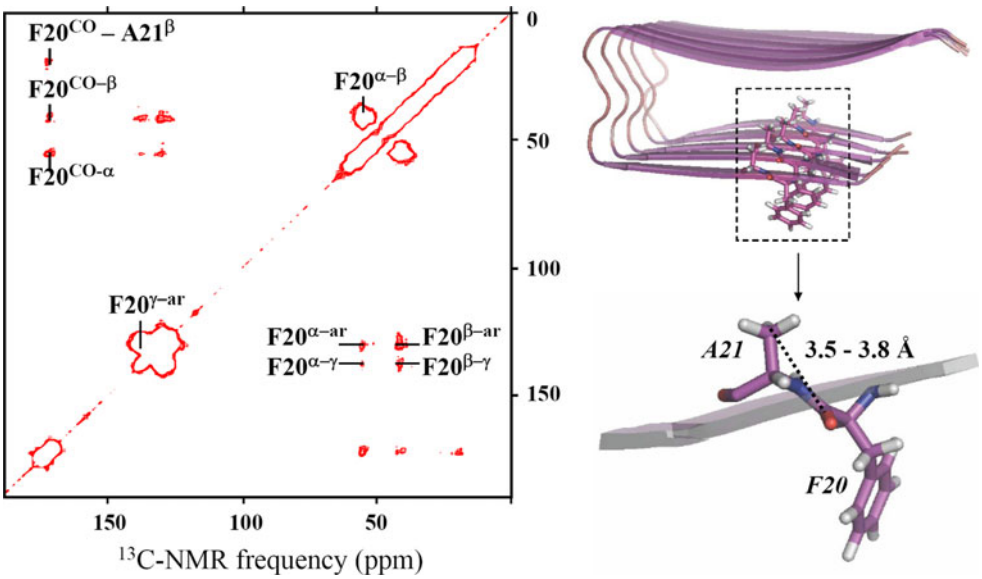

Fig. 6 PARIS-xy ^{13}C–^{13}C correlation spectrum of sample I, measured at 23.5 T (1,000 MHz for protons) and $\nu_{rot} = 52$ kHz, $m = 2$, $\nu_1^H = 30$ kHz, $\tau_m = 390$ ms, obtained with covariance processing. 42 complex points were sampled in the t_1 dimension ($t_1^{max} = 0.81$ ms) with 1,200 scans each and a recycle delay 2.8 s. The inter-residue distance between $F20^{CO}$ and $A21^{\beta}$ is highlighted in the structural model

Like in sample I, the transfer among aliphatic carbons, as well as between aliphatic and carbonyl carbons, permits one to distinguish two different conformations involving $F20^{\alpha}$ through four well separated cross-peaks $F20^{\alpha\text{-}CO}$, $F20C^{\alpha}*^{\text{-}CO}$, $F20^{\alpha-\beta}$ and $F20C^{\alpha}*^{\text{-}\beta}$, one of which, referred to as $F20^{\alpha}*$, having a small population hidden by the natural abundance signal in the 1D spectrum (Fig. 5). Under our experimental conditions, the original PARIS (Weingarth et al. 2008b, 2009a) sequence offers another option to transfer magnetization between spectrally close signals.

Figure 6 shows a PARIS-xy correlation spectrum recorded with $\nu_{rot} = 52$ kHz at the highest static field currently available (23.5 T or 1,000 MHz for protons). Besides broadband intra-residue transfer processes, the spectrum reveals an inter-residue contact between $F20^{CO}$ and $A21^{\beta}$ for a distance (Lührs et al. 2005) of 3.5–3.8 Å, corresponding to carbon–carbon dipole–dipole couplings between 177 and 138 Hz. Due to the much longer intermolecular distance between relevant residues, a contribution to the observed contact can be safely neglected regardless of the structural model. The cross peak has a relative intensity of about 2.8% compared to the diagonal peak of the $A21^{\beta}$. The observation of such a long-range transfer, which cannot be due to a relayed transfer since $A21^{\beta}$ is selectively ^{13}C-labelled, suggests that dipolar truncation, i.e., the quenching of magnetization transfer through small dipolar couplings by larger competing couplings, does not significantly affect PARIS-xy experiments. Dipolar truncation remains a considerable challenge, especially in uniformly labelled samples (Bayro et al. 2009a, b). The fact that PARIS-xy seems largely immune to dipolar truncation, like other methods that use only proton irradiation, results from the second-order nature of the transfer mechanism (Grommek et al. 2006; Scholtz et al. 2010). Indeed, in this case the magnetization transfer depends on residual couplings that are not averaged by MAS. These correspond to cross-terms between two dipolar couplings that have one spin in common (Grommek et al. 2006). First-order methods are more prone to dipolar truncation if the difference between two dipolar couplings is pronounced (Bayro et al. 2009a, b). The contact between the carbonyl $F20^{CO}$ and the methyl group $A21^{\beta}$ is particularly challenging, since the heteronuclear dipolar CH couplings are weak for both carbons. In addition, $F20^{CO}$ and $A21^{\beta}$ have a large chemical shift difference of 37.5 kHz at 1,000 MHz, which renders magnetization transfer even more challenging.

To probe to what extent PARIS-xy is sensitive to dipolar truncation, we carried out extensive numerical simulations for a model spin fragment $C^{\alpha}H^{\alpha}C^{\beta}H^{\beta}H^{\beta}H^{N}H^{N}CO$ based on the structural model of L-serine. Simulations were carried out assuming that the initial magnetization resided on C^{α} only. The graphs in Fig. 7 monitor the transfer of polarization from C^{α} to CO as a function of the distance $1.5 < r(C^{\alpha}\text{–CO}) < 4.0$ Å, either without C^{β} (blue dots) or with C^{β} (red squares), i.e., in the absence or presence of a dominant C^{α}–C^{β} dipolar coupling of 2 kHz. The simulations show that PARIS- xy is only weakly susceptible to dipolar truncation. Notably, the transfer efficiency reveals a linear dependence on the strength of the dipolar coupling, which would permit one to relate weak cross-peak intensities with long distances (see Fig. 3). The simulated C^{α}–CO transfer efficiency in the presence of C^{β} for a mixing time $\tau_m = 400$ ms over a range of distances $3 < r(C^{\alpha}\text{–CO}) < 4$ Å gives low intensity ratios $1.3 > R(C^{\alpha}\text{–CO}) > 0.6\%$, partly due to the limited size of the spin system considered in the simulations. To probe more closely the experimentally observed inter-residual contact

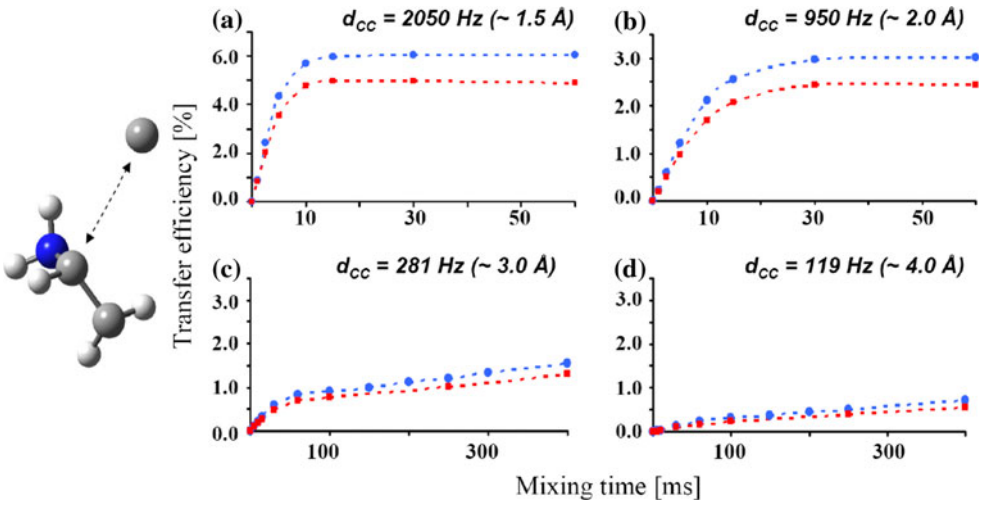

Fig. 7 Graphs that show the transfer of polarization from C^{α} to CO in a model 8-spin system $C^{\alpha}H^{\alpha}C^{\beta}H^{\beta}H^{\beta}H^{N}H^{N}CO$ based on a crystal structure of L-serine assuming distances **a** $r(C^{\alpha}–CO) = 1.5$ Å, **b** 2.0 Å, **c** 3.0 Å to **d** 4.0 Å without C^{β} (*blue dots*) and with C^{β} (*red squares*), i.e., in the absence and presence of a strong (2 kHz) $C^{\alpha}–C^{\beta}$ dipolar coupling

between $F20^{CO}$ and $A21^{\beta}$, further numerical simulations were carried out for a subsystem with $N = 9$ spins (Fig. S3) with a geometry based on a structural model of Aβ42 (Lührs et al. 2005) and under conditions close to the experimental ones ($\nu_1^H = 30$ kHz, $m = 2$, $\nu_{rot} = 50$ kHz, $\tau_m = 400$ ms, 23.5 T or 1,000 MHz for protons). Here again, the cross-peak intensity ratios of $F20^{CO}–A21^{\beta}$ (Fig. 8) without and with carbon $F20^{\alpha}$, which may cause dipolar truncation, differ merely by ~11%. This confirms the simulations using a model of L-serine, and corroborates the experimental observations that PARIS-xy is rather insensitive to dipolar truncation.

The transfer induced by PARIS-xy relies on residual dipolar couplings. Thus, its efficiency roughly scales with the inverse of the spinning frequency (Grommek et al. 2006), so that the fraction of transferred magnetization is small at very fast MAS. This in turn requires a good signal/noise ratio, which can be achieved at very high magnetic fields and with the help of covariance processing permitting to record more scans for each t_1 increment.

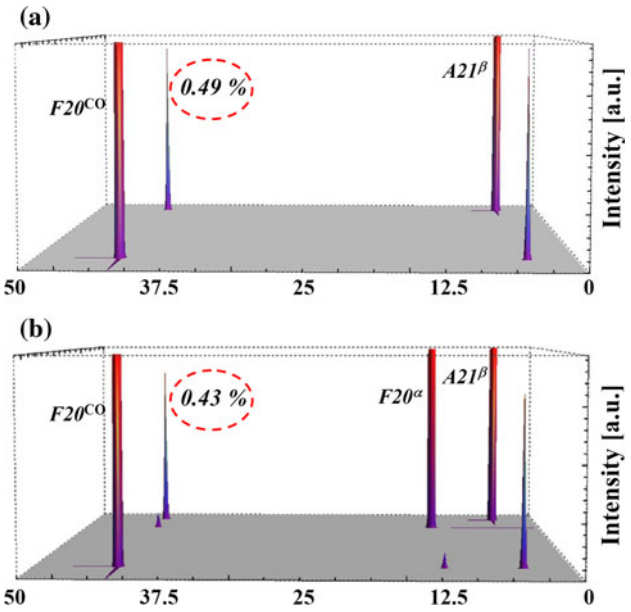

Fig. 8 Simulated PARIS-xy $^{13}C–^{13}C$ correlation spectrum of a model 9 spin fragment (see Supporting Material Figure S3) of the amyloid β (1–42) extracted from the structure model without (**a**) and with (**b**) a carbon-13 at position $F20^{\alpha}$. Note that the weak intensity of the intra-residual cross-peak $F20^{C\alpha}–F20^{CO}$ is due to the fact that the proton $F20^{H\alpha}$ was not included in the simulations

Conclusions

We have demonstrated that PARIS-xy recoupling using moderate *rf* amplitudes allows one to record sensitive 2D $^{13}C–^{13}C$ correlation spectra of amyloid β fibrils with as little as 1 mg of sample by promoting magnetization transfer even at very high spinning frequencies and magnetic fields up to 23.5 T. A moderate recoupling *rf* amplitude renders the PARIS-xy sequence particularly useful for heat-sensitive samples and allows one to use long mixing times. Furthermore, we have shown both experimentally and by numerical simulations that the method is not very sensitive to dipolar truncation effects and can reveal direct transfer across the distances 3.5–4 Å. Altogether, considering its ease of implementation, PARIS-xy may become an attractive tool for spectral assignment and for probing local geometries of biomolecular systems.

Acknowledgments Financial support from the Agence Nationale de la Recherche (ANR-09-BLAN-0111-01) and from the Fédération de Recherche (FR 3050) Très Grands Equipements de Résonance Magnétique Nucléaire à Très Hauts Champs (TGE RMN THC) of the CNRS is gratefully acknowledged. We thank Prof. Kazuhiro Irie at the Division of Food Science and Biotechnology, Graduate School of Agriculture, Kyoto University, for the use of a peptide synthesizer. We are grateful to Dr. Ken-ichi Akagi, Ms. Youko Monobe, and

Dr. Takayoshi Imazawa at Laboratory of Common Apparatus, Division of Biomedical Research, National Institute of Biomedical Innovation for obtaining electron micrographs.

References

Ahmed M, Davis J, Aucoin D, Sato T, Ahuja S, Aimoto S, Elliott JI, van Nostrand WE, Smith SO (2010) Structural conversion of neurotoxic amyloid-β1-42 oligomers to fibrils. Nat Struct Mol Biol 17:561–567

Bayro MJ, Maly T, Birkett NR, Dobson CM, Griffin RG (2009a) Long-range correlations between aliphatic C-13 nuclei in protein MAS NMR spectroscopy. Angew Chem Int Ed 48:5708–5710

Bayro MJ, Huber M, Ramachandran R, Davenport TC, Meier BH, Ernst M, Griffin RG (2009b) Dipolar truncation in magic-angle spinning NMR recoupling experiments. J Chem Phys 130:8

Cady SD, Schmidt-Rohr K, Wang J, Soto CS, DeGrado WF, Hong M (2010) Structure of the amantadine binding site of influenza M2 proton channels in lipid bilayers. Nature 463(7281):689–U127

Castellani F, van Rossum B, Diehl A, Schubert M, Rehbein K, Oschkinat H (2002) Structure of a protein determined by solid-state magic-angle-spinning NMR spectroscopy. Nature 420:98–102

Chimon S, Shaibat MA, Jones CR, Calero DC, Aizezi B, Ishii Y (2007) Evidence of fibril-like beta-sheet structures in a neurotoxic amyloid intermediate of Alzheimer's beta-amyloid. Nat Struct Mol Biol 14(12):1157–1164

Grommek A, Meier BH, Ernst M (2006) Distance information from proton-driven spin diffusion under MAS. Chem Phys Lett 427:404–409

Irie K, Oie K, Nakahara A, Yanai Y, Ohigashi H, Wender PA, Fukuda H, Konishi H, Kikkawa U (1998) Molecular basis for protein kinase C isozyme-selective binding: the synthesis, folding, and phorbol ester binding of the cysteine-rich domains of all protein kinase C isozymes. J Am Chem Soc 120:9159–9167

Iwata K, Fujiwara T, Matsuki Y, Akutsu H, Takahashi S, Naiki H, Goto Y (2006) 3D Structure of amyloid protofilaments of b2-microglobulin fragment probed by solid-state NMR. Proc Natl Sci USA 103:18119–18124

Laage S, Sachleben JR, Steuernagel S, Pierattelli R, Pintacuda G, Emsley L (2009) Fast acquisition of multi-dimensional spectra in solid-state NMR enabled by ultra-fast MAS. J Magn Reson 196:133–141

Lange A, Becker S, Seidel K, Giller K, Pongs O, Baldus M (2005) A concept for rapid protein-structure determination by solid-state NMR spectroscopy. Angew Chem Int Ed 44:2089–2092

Lange A, Giller K, Hornig S, Martin-Eauclaire MF, Pongs O, Becker S, Baldus M (2006) Toxin-induced conformational changes in a potassium channel revealed by solid-state NMR. Nature 440(7086):959–962

Lührs T, Ritter C, Adrian M, Riek-Loher D, Bohrmann B, Döbeli H, Schubert D, Riek R (2005) 3D structure of Alzheimer's amyloid-beta (1–42) fibrils. Proc Natl Sci USA 102:17342–17347

Masuda Y, Nakanishi A, Ohashi R, Takegoshi K, Shimizu T, Irie K (2008) Verification of the intermolecular parallel β-sheet in E22K-Aβ42 aggregates by solid-state NMR using rotational resonance: implications for the supramolecular arrangement of the toxic conformer of Aβ42. Bios Biotechnol Biochem 72:2170–2175

Masuda Y, Uemura S, Ohashi R, Nakanishi A, Takegoshi K, Shimizu T, Shirasawa T, Irie K (2009) Identification of physiological and toxic conformations in Aβ42 aggregates. Chem BioChem 10:287–295

Murakami K, Irie K, Morimoto A, Ohigashi H, Shindo M, Nagao M, Shimizu T, Shirasawa T (2002) Synthesis, aggregation, neurotoxicity, and secondary structure of various A beta 1-42 mutants of familial Alzheimer's disease at positions 21-23. Biochem Biophys Res Commun 294:5–10

Nielsen JT, Bjerring M, Jeppesen MD, Pedersen RO, Pedersen JM, Hein KL, Vosegaard T, Skrydstrup T, Otzen DE, Nielsen NC (2009) Unique identification of supramolecular structures in amyloid fibrils by solid-state NMR spectroscopy. Angew Chem Int Ed 48:2118–2121

Petkova AT, Ishii Y, Balbach JJ, Antzutkin ON, Leapman RD, Delaglio F, Tycko R (2002) A structural model for Alzheimer's beta-amyloid fibrils based on experimental constraints from solid state NMR. Proc Natl Sci USA 99(26):16742–16747

Petkova AT, Leapman RD, Guo ZH, Yau WM, Mattson MP, Tycko R (2005) Self-propagating, molecular-level polymorphism in Alzheimer's beta-amyloid fibrils. Science 307:262–265

Potrzebowski MJ, Tekely P, Dusausoy Y (1998) Comment to ^{13}C NMR studies of α and γ polymorphs of glycine. Solid State NMR 11:253–257

Rienstra CM, Tucker-Kellogg L, Jaroniec CP, Hohwy M, Reif B, McMahon MT, Tidor B, Lozano-Perez T, Griffin RG (2002) De novo determination of peptide structure with solid-state magic-angle spinning NMR spectroscopy. Proc Natl Sci USA 99:10260–10265

Scholz I, van Beek JD, Ernst M (2010) Operator-based Floquet theory in solid-state NMR. Solid State Nucl Mag Reson 37:39–59

Sperling LJ, Nieuwkoop AJ, Lipton AS, Berthold DA, Rienstra CM (2010) High resolution NMR spectroscopy of nanocrystalline proteins at ultra-high magnetic field. J Biomol NMR 46:149–155

Tycko R (2006) Molecular structure of amyloid fibrils: insights from solid-state NMR. Q Rev Biophys 39:1–55

Veshtort M, Griffin RG (2006) SPINEVOLUTION: a powerful tool for the simulation of solid and liquid state NMR experiments. J Magn Reson 178:248–282

Weingarth M, Tekely P, Bodenhausen G (2008a) Efficient heteronuclear decoupling by quenching rotary resonance in solid-state NMR. Chem Phys Lett 466:247–251

Weingarth M, Demco DE, Bodenhausen G, Tekely P (2008b) Improved magnetization transfer in solid-state NMR with fast magic angle spinning. Chem Phys Lett 469:342–348

Weingarth M, Bodenhausen G, Tekely P (2009a) Broadband carbon-13 correlation spectra of microcrystalline proteins in very high magnetic fields. J Am Chem Soc 131:13937–13939

Weingarth M, Bodenhausen G, Tekely P (2009b) Low-power decoupling at high spinning frequencies in high static fields. J Magn Reson 199:238–241

Weingarth M, Bodenhausen G, Tekely P (2010a) Broadband magnetization transfer using moderate radio-frequency fields for NMR with very high static fields and spinning speeds. Chem Phys Lett 488:10–16

Weingarth M, Tekely P, Brüschweiler R, Bodenhausen G (2010b) Improving the quality of 2D solid-state NMR spectra of microcrystalline proteins by covariance analysis. Chem Comm 46:952–954

Weingarth M, Bodenhausen G, Tekely P (2011) Probing the quenching of rotary resonance by PISSARRO decoupling. Chem Phys Lett 502:259–265